Oscillatory Shear Flow-Induced Alignment of Lamellar Melts of Hydrogen-Bonded Comb Copolymer Supramolecules

Karin de Moel,[†] Riikka Mäki-Ontto,[‡] Manfred Stamm,[§] Olli Ikkala,*[,‡] and Gerrit ten Brinke*[,†]

Department of Polymer Science and Materials Science Center, Dutch Polymer Institute, University of Groningen, Nijenborgh 4, 9747 AG Groningen, The Netherlands; Department of Engineering Physics and Mathematics, Helsinki University of Technology, P.O. Box 2200, FIN-02015 HUT, Espoo, Finland; and Institut für Polymerforschung, D-01069 Dresden, Germany

Received August 11, 2000

ABSTRACT: In this work we present the orientational behavior of comb copolymer-like supramolecules P4VP(PDP)$_{1.0}$, obtained by hydrogen bonding between poly(4-vinylpyridine) and pentadecylphenol, during large-amplitude oscillatory shear flow experiments over a broad range of frequencies (0.001–10 Hz). The alignment diagram, presenting the macroscopic alignment in T/T_{ODT} vs ω/ω_c, contains three regions of parallel alignment separated by a region of perpendicular alignment. For our material, the order–disorder temperature $T_{ODT} = 67$ °C and ω_c, the frequency above which the distortion of the chain conformation dominates the materials' viscoelasticity, is around 0.1 Hz at 61 °C. For the first time flipping from a pure transverse alignment via biaxial transverse/perpendicular alignment to a perpendicular alignment as a function of the strain amplitude was found.

1. Introduction

1.1. Local Nanoscale Structures vs Overall Order. Methods to achieve nanoscale structuring of organic and inorganic materials have been under intense research during recent years[1] due to their possible applications in optics, electronics, engineering, and biosciences. Popular options include block copolymers of different architecture,[2–4] liquid crystalline polymers,[5] and even their combinations.[6] In general, the alignment of the nanoscale order is only local, and additional mechanisms to obtain macroscopic alignment have to be invoked, for example by imposing oscillatory flow. In this context, the flow properties of block copolymers have been studied extensively,[7–27] and a clear picture of the conditions that cause the different alignments of the lamellar order vs shear flow direction has emerged.[10–14,23–25] Shear flow can also be used to provide overall alignment of liquid crystalline materials including side chain liquid crystalline polymers.[28–30] Here it presents an option to achieve overall orientation in thick samples in contrast to electric[31] or magnetic fields,[32,33] which are applicable in thin films.

Recently, a new scheme to achieve nanostructures was introduced, based on supramolecular chemistry, where matching physical bonds are used to connect hosts and guests.[34] In this way physically bonded *supramolecules* are constructed, which behave much in the same way as classical covalently bonded molecules provided the physical bonds are sufficiently strong. In particular, the concept can be applied to achieve amphiphilic polymeric supramolecules which self-organize like block copolymers. Most of the examples studied so far have dealt with the comb architecture in which the side chains are either hydrogen bonded to the backbone[35–37] or bonded by ionic interactions.[38,39] For ex-

ample, a supramolecule can be constructed consisting of a poly(4-vinylpyridine), P4VP, backbone to which a stoichiometric amount of pentadecylphenol side chains are hydrogen bonded, leading to supramolecules which will be denoted as P4VP(PDP)$_{1.0}$. Such hydrogen-bonded supramolecules self-organize in analogy with ordinary comb copolymers—in this particular case in the form of a lamellar morphology with a long period of 36 Å (see Figure 1), with an order–disorder transition at ca. 67 °C, and shear moduli which scale as a function of the frequency similar to diblock copolymers.[35–37] Furthermore, our preliminairy study showed that the nanoscale structures can be macroscopically aligned by oscillatory shear flow.[40]

In this article we will investigate in more detail the behavior under oscillatory shear flow of such comb-shape supramolecules and construct a so-called alignment diagram, which maps the macroscopic alignment of the lamellar self-organized structure as a function of the oscillation parameters: (reduced) temperature, (reduced) frequency, time, and strain amplitude. Before describing our findings, we will first summarize the pertinent results from experiments on diblock copolymers and liquid crystals including side chain liquid crystalline polymers.[14,15,19,20,24,28–30,41–46] These will be compared with the observed results for P4VP(PDP)$_{1.0}$ and will be used to gain insight into the mechanisms underlying the orientational behavior in the different frequency regimes of the alignment diagram.

1.2. Shear Flow Properties of Diblock Copolymers and Side Chain Liquid Crystalline Polymers. Diblock copolymers and side chain liquid crystalline polymers have related properties: they form nanoscale structures, they can be shear oriented, and the shear moduli depend similarly on the oscillation time and on the frequency in the linear regime.[29] Therefore, it was suggested that the same processes determine the shear orientation behavior regardless of whether the nanoscale structures are formed due to competition between attraction and repulsion (in self-organization) or due to
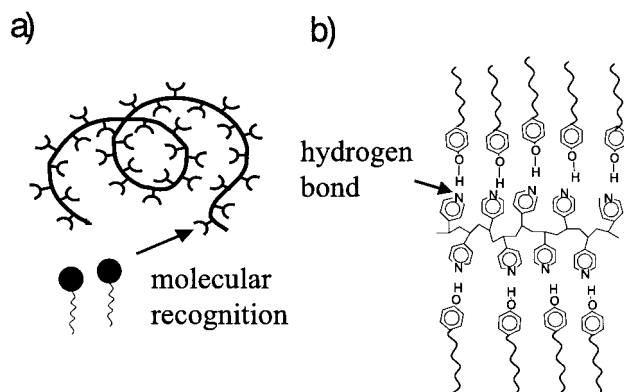
Figure 1. Schematics of the supramolecular comb copolymer P4VP(PDP)$_{1.0}$. Comb-shape supramolecules are formed by connecting pentadecyl alkyl tails contained in pentadecylphenol (PDP) using phenolic hydrogen bonds to the pyridine groups of P4VP. (a, b) A simple hydrogen bonding suffices to achieve a strong enough physical bond, and more complicated recognition is not needed. (c) The supramolecules, in turn, self-organize as lamellae with a long period of $L_p \approx 36$ Å.

excluded-volume effects of rigid mesogenic moieties (in liquid crystals).

Our comb-shape supramolecules share a number of features with both materials. They have an architecture that is similar to comb copolymers and side chain liquid crystalline polymers. The smectic A phase of these materials is characterized by side chains that are oriented perpendicular to the layers containing the polymer backbones. In the case of diblock copolymers, on the other hand, both blocks are oriented perpendicular to the interface. Still, the functional dependence of the shear moduli G' and G'' on frequency ω of our comb-shape supramolecules was found to be the same as for linear diblock copolymers.[36] Above the order−disorder transition (ODT) slopes of respectively 1.0 and 2.0 for log G'' and log G' vs log ω are found, whereas below the ODT the slope is approximately equal to 0.5 for both moduli.[3,36,47] Despite the structural and rheological analogies with side chain liquid crystalline polymers and block copolymers, the comb-shape supramolecules might respond differently to the applied oscillatory flow, due to the reversibility of the hydrogen bonds connecting the side chains and the backbone.

Diblock Copolymers. The shear alignment behavior of lamellar diblock copolymers has been studied thoroughly as a function of the frequency, strain amplitude, temperature, time, and block length.[10,11,14−16,19−21,23,24,41,42,48−50] For convenience, the pertinent results have been summarized in Figure 2, where the frequency is scaled by ω_c, corresponding to the longest relaxation time of the polymer chains. Four different regimes can be distinguished,[24] in which the lamellae align either parallel (regions B, C, and D) or perpendicular (region A) (Figures 2 and 3). Parallel alignment corresponds to the unit vector normal to the layers $\hat{n}$ pointing along the velocity gradient $\nabla \mathbf{v}$ direction. In the case of perpendicular orientation, $\hat{n}$ points along the vorticity axis $\nabla \times \mathbf{v}$. For PS-*block*-PI, the low-frequency parallel alignment (D) was only found after prolonged annealing.[21,51] For PEE-*block*-PEP, the high-frequency parallel alignment (B and C) was absent, due to the lack of so-called viscoelastic contrast between the two blocks.[10,14] The transverse alignment, corresponding to $\hat{n}$ being parallel to $\mathbf{v}$ (Figure 3c), proved to be metastable and was only found as an intermediate stage
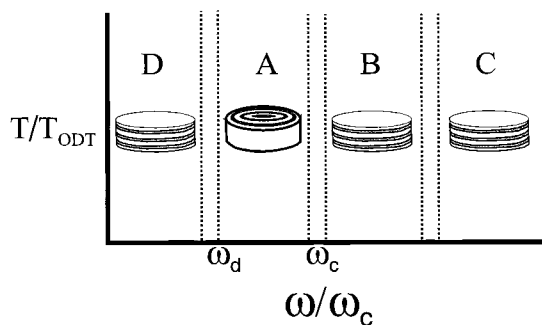
Figure 2. Alignment diagram of diblock copolymers as a function of reduced temperature (T/T_{ODT}) and reduced frequency (ω/ω_c').[24] In regions B, C, and D the alignment is parallel and in region A perpendicular as indicated. The crossover frequency between region A and D is generally called ω_d, the frequency below which the relaxation of the domains becomes significant. ω_c is the frequency above which the distortion of the chain comformations dominates the viscoelastic properties. In the region between A and B, flipping of orientation as a function of the strain amplitude was observed.[25] In region D, PS-*block*-PI showed perpendicular alignment without prolonged annealing.[12,56] Regions B and C were absent for PEP-*block*-PEE polymers.[10,14]
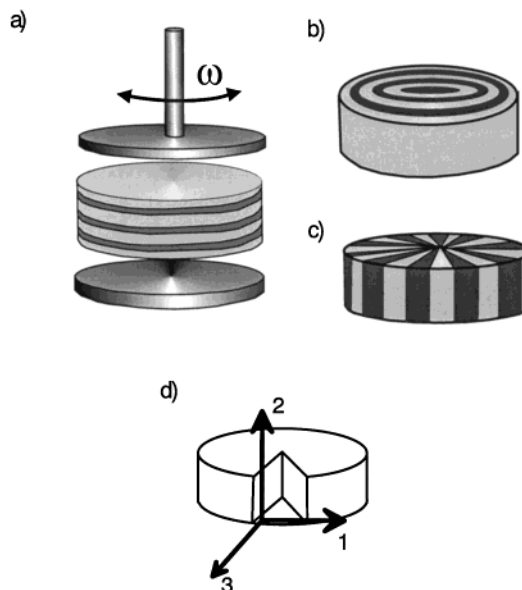
Figure 3. Schematics of the possible alignments of lamellar structures upon application of large-amplitude oscillatory shear flow between two plates: (a) lamellae with the normal along the 2-direction: parallel alignment; (b) lamellae with the normal along the 3-direction: perpendicular alignment; and (c) lamellae with the normal along the 1-direction: transverse alignment. The directions are shown in (d).

en route to parallel alignments in regime C. All other trajectories passed through a biaxial parallel/perpendicular alignment, although in each regime different mechanisms play a role.[15,19,20,24,41]

The transition from region A to D takes place around a characteristic frequency ω_d, defined as the frequency below which the domains have sufficient time to respond to the applied oscillatory flow.[10,11,21,48] Two methods have been used to evaluate ω_d: it can be assessed from the slope of the dynamic viscosity or of tan δ vs the frequency[16,17,23,51] or from a small bump in the storage modulus in the shear plane (G_{xy}').[10]

Variation of the strain amplitude at a fixed frequency can lead to a flip in orientation,[21,25] especially at the border between the regions A and B. A different type of

diagram has also been constructed, where the strain amplitude instead of the temperature is plotted against the frequency.[21,48] Lines of more or less constant frequency times strain amplitude separate the three regimes.

Prolonged oscillatory flow using low strain amplitudes gave similar results as short oscillatory flow using higher amplitudes.[16] This implies a functional dependence between the time and the strain amplitude, but a single dimensionless time could not be used to describe the alignment kinetics in a single trajectory, let alone the whole alignment diagram.[41]

Side Chain Liquid Crystalline Polymers. Shear flow has also been applied to achieve orientation of surfactant membranes, smectic lamellar phases of low molecular thermotropic liquid crystals, and smectic phases of side chain liquid crystalline polymers.[28–30,44,46,52,53] Hamley et al.[30] observed a perpendicular orientation ($\hat{n}$ parallel to $\nabla \times \mathbf{v}$) in the case of large-amplitude oscillatory shear flow applied to the smectic phase of a side chain liquid crystal polymer. For a similar system a parallel orientation ($\hat{n}$ parallel to $\nabla\mathbf{v}$) was found in the case of steady shear (see Figure 3a,b).[53]

2. Experimental Section

Materials and Sample Preparation. Poly(4-vinylpyridine), P4VP, was obtained from Polyscience Inc. with $M_n = 50\,000$ g/mol. 3-n-Pentadecylphenol, PDP, was purchased from Aldrich (purity 98%). It was twice recrystallized with pethrol ether and dried at 40 °C in a vacuum for 4 days. Comb-shape supramolecules were prepared by mixing P4VP and a stoichiometric amount of PDP (with respect to the number of pyridine groups) in a dilute solution of analysis grade chloroform. At the end, chloroform was evaporated and the sample was vacuum-dried. From the previous work it is known that such P4VP(PDP)$_{1.0}$ has an order–disorder transition (ODT) temperature of ca. 67 °C, above which it is disordered and below which it has lamellar order.[36] Other details of sample preparation have been described elsewhere, also describing the preparation of the sample pills for the rheology.[40]
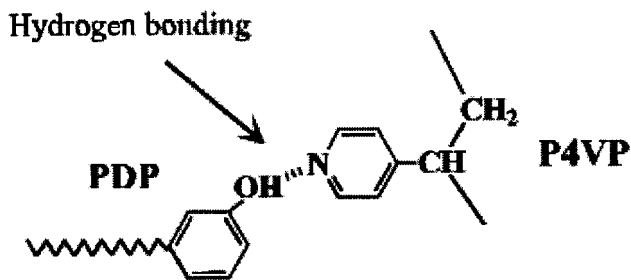
Dynamic Rheology. The rheological properties were measured in an oscillating mode by a Haake constant stress rheometer and a Bohlin VOR rheometer, using a plate–plate geometry with plate diameters of 60 and 25 mm, respectively, and a gap of 1.0 mm. First the samples were shortly heated to 80 °C, which is well above the ODT, to erase all history and to obtain a homogeneous sample with good contact with the rotor and the stator of the rheometer.

Small-Angle X-ray Scattering. After imposing shear flow, the samples were cooled to room temperature (i.e., below T_{ODT}) and removed from the rheometer, and the resulting structure was inspected with small-angle X-ray scattering (SAXS) using a Bruker NanoSTAR, which consists of a Kristalloflex K760-8 3.0 kW X-ray generator with cross-coupled Göbel mirrors for Cu Kα radiation ($\lambda = 1.54$ Å) resulting in a parallel beam of about 0.05 mm² at the sample position. A Siemens multiwire type area detector was used. The sample–detector distance was 0.65 m. The SAXS intensity patterns were measured at room temperature in tangential, normal, and radial views, i.e.,
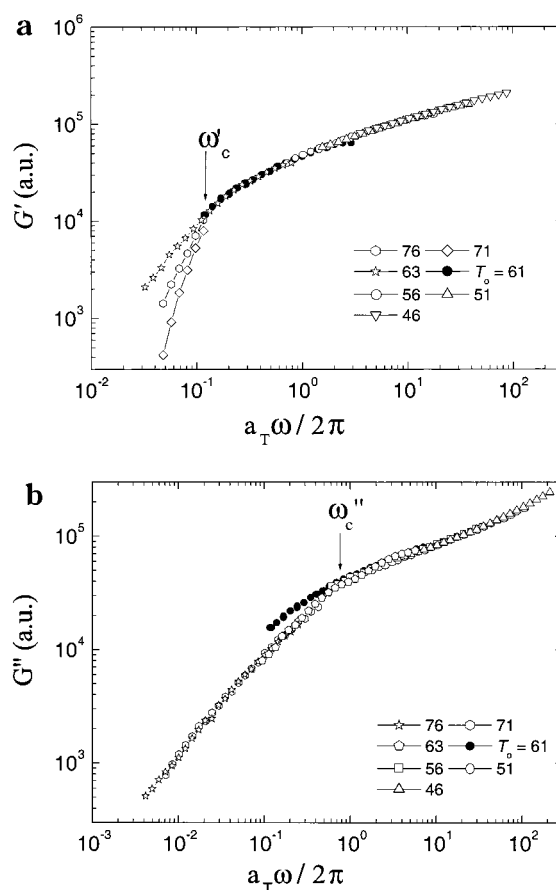
Figure 4. Master curves of (a) storage G' and (b) loss G'' moduli, obtained by time–temperature superposition, with $T_0 = 61$ °C (solid dots). From (a) ω_c' is around 0.1 Hz; from (b) ω_c'' is around 1.0 Hz.

with the incident beam along the 1-, 2-, and 3-direction, respectively (see Figure 3d). Samples were measured in the rim, i.e., where the strain is highest. The structures were compared to those measured before the imposed shear.

Construction of the Alignment Diagram. Large-amplitude oscillatory shear experiments were carried out at a broad range of frequencies, 0.001–10 Hz, and three different temperatures, 65, 63, and 56 °C, which is respectively 2, 4, and 11 deg below the T_{ODT} measured in the present samples (67 °C). At all frequencies a strain amplitude of 100% was used. Additional oscillation was performed at 0.01 Hz at 1%, 20%, and 40% strain amplitudes and at 1.0 Hz at 60% strain amplitude. The crossover from the linear regime to the nonlinear regime occurred at a strain amplitude of approximately 10% at 1.0 Hz. Unless otherwise stated, all oscillation experiments refer to a strain amplitude of 100%.

3. Results

3.1. Determination of the Critical Frequencies. First the frequency ω_c is determined from both the G' and G'' data, to allow two estimates, i.e., ω_c' and ω_c'', respectively. Therefore, master curves of G' and G'' were constructed on the basis of time–temperature superposition using a reference temperature $T_0 = 61$ °C (see Figure 4a,b). The WLF equation describes the shift factors in the ordered region, with $C_1 = -6$ and $C_2 = 11$ for G' and $C_1 = -7$ and $C_2 = 18$ for G''. For the latter case, an Arrhenius type fit could also be used, with an activation energy of 27 kJ/mol. Similar results have been obtained for side chain liquid crystalline polymers.[29]

Below the ODT, G' and G'' behave as $\omega^{1/2}$, whereas in the disordered phase above the ODT we find $G' \propto \omega^2$

and $G'' \propto \omega$, in agreement with previous work.[36] This corresponds to the usual result for lamellar ordered diblock copolymers.[4,36,47] The loci of ω_c' around 0.1 Hz and of ω_c'' around 1.0 Hz are indicated by arrows in Figure 4. We were unable to determine ω_d based on our data.

3.2. The Alignment Diagram. The alignment diagram, i.e., T/T_{ODT} vs ω/ω_c, has been determined by imposing oscillations over a broad range of frequencies (0.001–10 Hz) at three different temperatures, namely, 56, 63, and 65 °C. All data are time–temperature shifted to $T_0 = 61$ °C.

Low Frequencies: Parallel, Transverse, and Perpendicular Alignments. Using low-frequency (0.01 Hz) and low-amplitude (1%) oscillations at 63 °C for 9.8 h, the lamellae aligned with their normal in the 1-direction, i.e., transverse, as is clear from the peaks in the normal and radial views in Figure 5. The material was well aligned, and no traces of other alignments were present. In this case the side chains, accounting for 75% of the material, are oriented parallel to **v**. Upon increasing the strain amplitude from 20% to 100%, the intensity maxima corresponding to transverse alignment are slowly replaced by peaks in the 3-direction in tangential and normal views, i.e., those corresponding to perpendicular alignment. This is clear from Figure 6, where the azimuthal projections of the scattering intensity in all three views for the 20%, 40%, and 100% strain amplitudes are displayed. Even at 100% strain amplitude, regions with transversely aligned lamellae were still present.

In addition to 0.01 Hz at 63 °C, the material was sheared using still lower frequencies to test whether the transverse orientation might become stable for large strain amplitudes at lower frequencies. If this would be the case, the results obtained at 0.01 Hz at 63 °C would demonstrate a border between a region with perpendicular alignment at higher frequencies and a region with transverse alignment at lower frequencies. However, as Figure 7 shows, after 92 h of shearing at 0.001 Hz and 100% strain amplitude at 63 °C, the material was mainly aligned parallel. It still contained isotropic regions, probably because the frequency was so low. This experiment shows that at very low frequencies the dominant alignment is parallel instead of transverse.

The results from 0.01 Hz show the stable alignment at this frequency range for sufficiently large amplitudes to be perpendicular. This was confirmed by experiments at 0.5 Hz at 65 °C for 18 h and at 0.5 Hz at 63 °C for 27 h. The SAXS intensities in all three views of the former are displayed in Figure 8, showing no trace of transverse alignment.

Intermediate Frequencies: Parallel and Perpendicular Alignments. The frequencies used in this regime were 0.5 Hz (56 °C) and 1.0 Hz (63 and 56 °C). To investigate the effect of time as well, three experiments were carried out at 0.5 Hz: for 0.2 h, for 6.5 h, and for 15 h. Figure 9 shows the azimuthal projection of the scattering intensity in the tangential, normal, and radial views for these three experiments. Remarkably, after 0.2 h the material was aligned parallel, as is clear from the sharp peaks in the 2-direction in the tangential and radial views. After 6.5 h the intensity in the 2-direction was reduced, and additional peaks in the 3-direction appeared in the tangential and normal views. The material was biaxially perpendicular and parallel aligned. After 15 h, however, the peaks in the 3-direction were
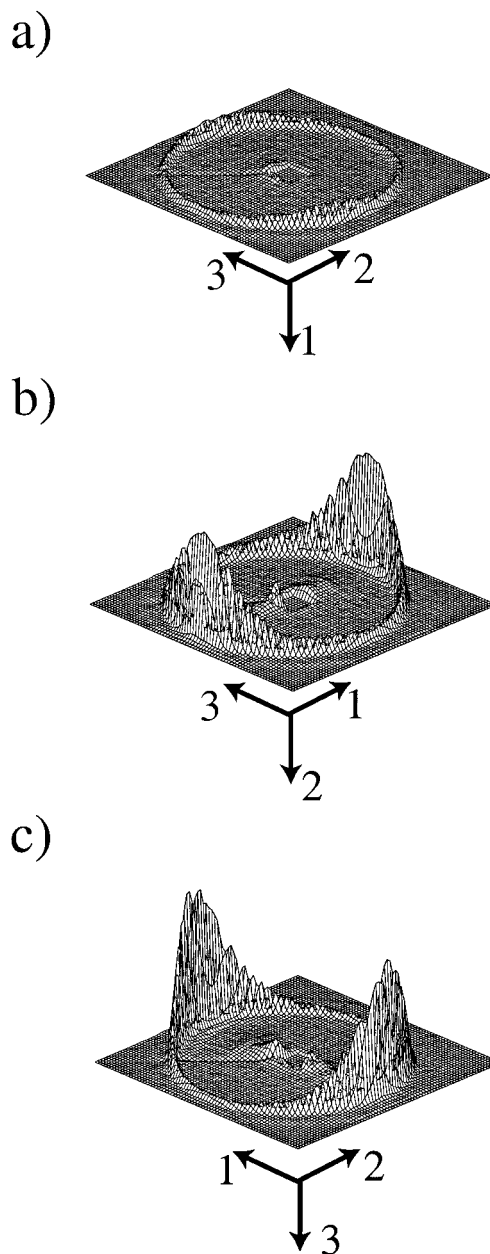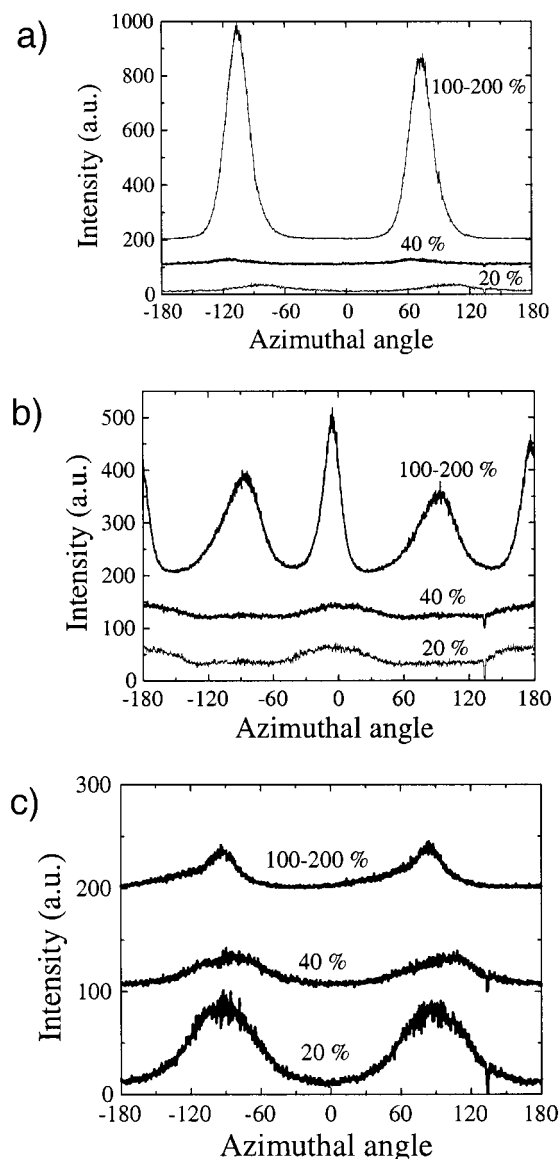

Figure 5. SAXS intensities in (a) tangential, (b) normal, and (c) radial views of P4VP(PDP)$_{1.0}$ after shearing at 0.01 Hz, 63 °C, and 1% strain amplitude for 9.8 h. The downward arrow in each figure denotes the direction of the incident beam. The large peaks in normal and radial views show that the lamellae are oriented with their normal along the 1-direction, i.e., transverse.

decreased, and mainly parallel aligned regions remained (see Figures 9 and 10).

A similar flipping as a function of time occurred using 1.0 Hz and 60% strain amplitude at 63 °C, where after 3.5 h the orientation was predominantly perpendicular but proved to be parallel after 5.1 h. These results show that not only temperature and frequency have a pronounced effect on the orientation behavior of P4VP-(PDP)$_{1.0}$, time plays an important role, too.

High Frequencies: Parallel Alignment. Experiments were carried out at 10 Hz at 65 °C for 6.5 h and at 56 °C for 22 h. All resulted in predominantly parallel alignments; the latter had also regions of transversely oriented lamellae (see Figure 11). When time–temperature shifted to 61 °C, the first experiment at 65 °C

Figure 6. Azimuthal projections of the SAXS intensities of three oscillation experiments at 0.01 Hz and 63 °C respectively at 20%, 40%, and 100% strain amplitudes in (a) tangential, (b) normal, and (c) radial views. At 20% there are clear peaks present at ±90° in the radial view (c) and small peaks at 0° and 180° in the normal view (b), i.e. in the 1-direction, corresponding to transverse alignment. At strain amplitudes of 40% and 100% these peaks are still present in both views; at 40% they are less high. At 100% the higher intensities at ±90° in (a) and (b) show the dominant alignment to be perpendicular.

turned out to be in the intermediate frequency regime (see Figure 12). The second at 56 °C, however, clearly shows that at frequencies much larger than ω_c' parallel alignment can be found. The route toward final parallel alignment seems different at 10 Hz compared to 0.5 Hz as indicated by the presence of transversely oriented lamellae. Therefore, we believe to have probed a second region of parallel alignment at high frequencies.[24]

The Alignment Diagram. Summarizing, we can distinguish four different frequency regimes in the alignment diagram of P4VP(PDP)$_{1.0}$, numbered I to IV in Figure 12. The alignment for this material is either parallel (region IV, II, and III) or perpendicular (region I). The points in the figure correspond to the experiments mentioned above, time–temperature shifted to $T_0 = 61$ °C. The crossover from region I to region II
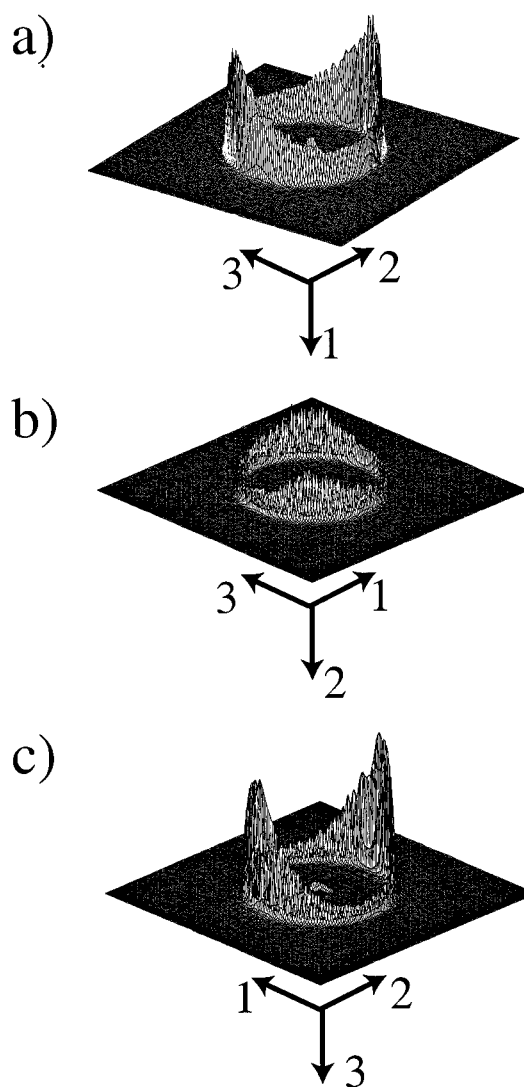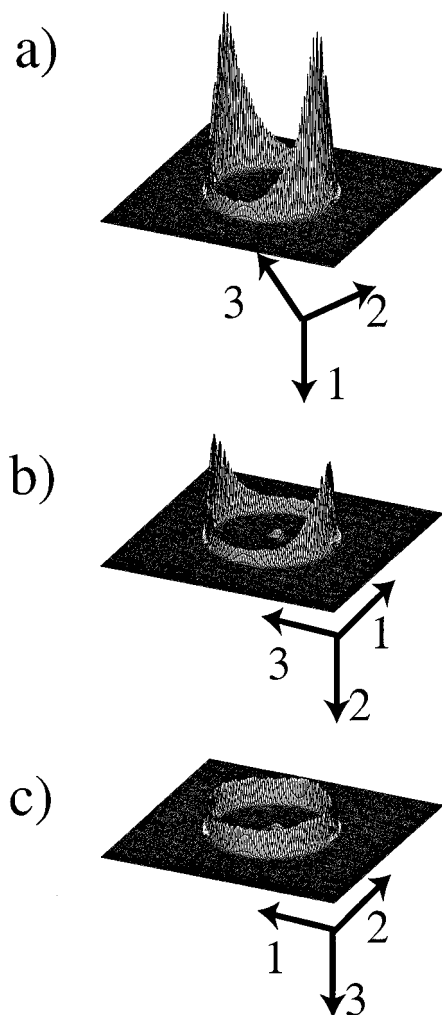

Figure 7. SAXS intensities in (a) tangential, (b) normal, and (c) radial views after oscillating P4VP(PDP)$_{1.0}$ for 92 h at 0.001 Hz, 63 °C, and 100% strain amplitude. Peaks in (a) and (c) in the 2-direction indicate parallel alignment. The large background intensity in (a) indicates that isotropic regions are still present, likely due to the low frequency.

occurs near ω_c', which is around 0.1 Hz. The crossover between region IV and I occurs near 4×10^{-3} Hz. This frequency most likely corresponds to ω_d of our system, the frequency below which the relaxation of the domains becomes significant.

4. Discussion

4.1. Comparison with Results from Diblock Copolymers. The alignment diagram, as shown in Figure 12, has similarities to that of the PS-*block*-PI diblock copolymers.[24] As illustrated in Figure 2, PS-*block*-PI also has a low-frequency perpendicular (A) and higher-frequency parallel alignments (B and C).[24] The low-frequency parallel alignment (region D) was only found for annealed PS-*block*-PI diblock polymers[51] and for PEP-*block*-PEE diblock copolymers,[10,14] where the regions B and C are absent. For P4VP(PDP)$_{1.0}$, which can be regarded as a supramolecular comb copolymer, however, the low-frequency parallel region (IV) was found without annealing the material, which might be due to the fact that P4VP(PDP)$_{1.0}$ can also be regarded as a polymer/solvent complex with faster relaxations.
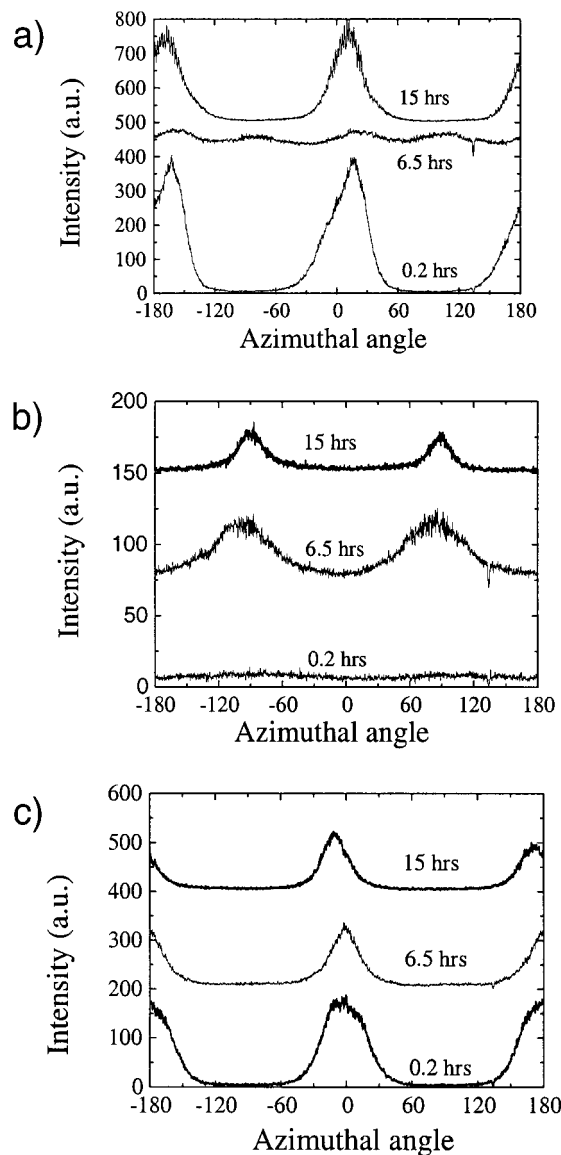
Figure 8. SAXS intensities in (a) tangential, (b) normal, and (c) radial views after oscillation for 27 h at 0.5 Hz, 63 °C, and 100% strain amplitude. Tangential (a) and normal (b) views show sharp peaks in the 3-direction, corresponding to perpendicular alignment. The material still contains isotropic regions, as the large background in all three views indicates.

In agreement with PS-*block*-PI,[19] we also found transverse alignment present at $\omega \gg \omega_c$ (III) and biaxial parallel/perpendicular alignments at frequencies close to but above ω_c in the intermediate frequency regime (II).

In the case of PS-*block*-PI close to T_{ODT} and above ω_c flipping of the alignment as a function of strain amplitude was observed.[21,25] Low amplitudes promoted parallel alignment, whereas high amplitudes led to perpendicular alignment. For P4VP(PDP)$_{1.0}$ a similar kind of flipping was observed in region I, where low amplitudes induced transverse alignment and high amplitudes led to perpendicular alignment.

The transverse alignment plays a dominant role in region I. A pure transverse alignment was found in the linear regime at 0.01 Hz and 1% strain (see Figure 5). Alignments with similar strain amplitudes have been reported for block copolymers.[12] A less well oriented transverse alignment for PS-*block*-PI with a similar molecular weight has also been reported.[16] In this case the shearing was performed, however, in the high-frequency limit (region A), where transverse alignment is metastable.[15,19,20,24,41]

Increasing the strain amplitude in the nonlinear regime of region I, biaxial perpendicular/transverse

Figure 9. Azimuthal projection of the SAXS intensities after oscillating at 0.5 Hz, 56 °C, and 100% strain amplitude with various shearing in (a) tangential, (b) normal, and (c) radial views. The small tilt in the curve corresponding to 15 h is not real but due to the experimental setup. The decrease and again increase of the peaks corresponding to parallel alignment in (a) and (c) at 0° and 180° shows that the material is sensitive to the applied shear time and that toward the perfect alignment one may pass through a less ordered state. This state contains perpendicularly aligned regions, as the presence of peaks at ±90° indicate.

alignments were found en route to the final perpendicular alignment. This means that the trajectory toward the final alignment, and thus the underlying mechanism, is different from that of PS-*block*-PI, where parallel alignment proved to be metastable.[24] Although biaxial perpendicular/parallel alignments have been reported for diblock copolymers,[21,50,54,55] to our knowledge this is the first time a biaxial transverse/perpendicular alignment has been found. The effect of increased strain amplitude seems comparable with an increase of the oscillating time, as reported before in the case of block copolymers.[16] Our experiments at 0.01 Hz support this hypothesis (see Figure 6).

4.2. Comparison with Results from Side Chain Liquid Crystalline Polymers. A quantitative comparison of the results summarized in Figure 12 with the
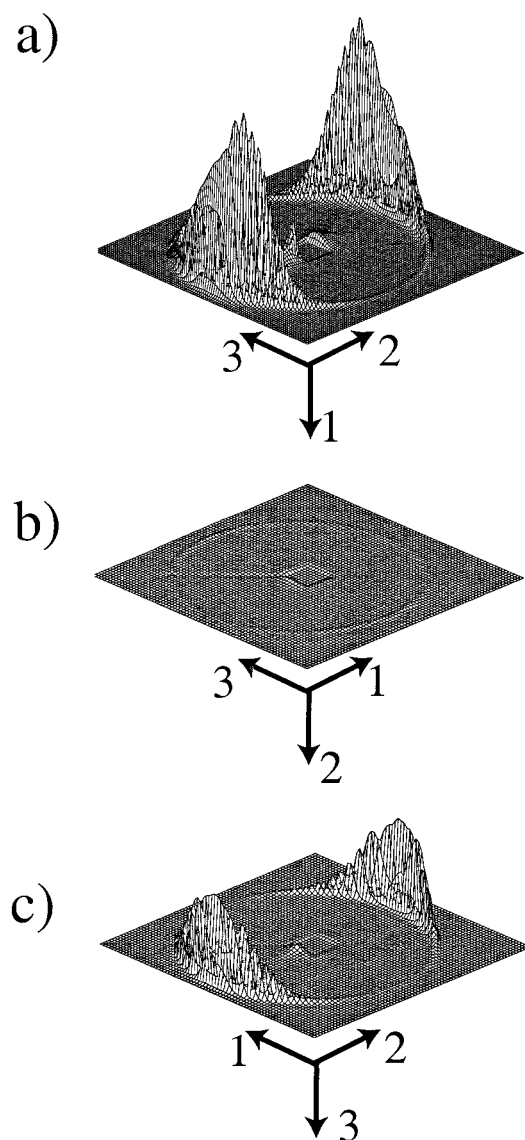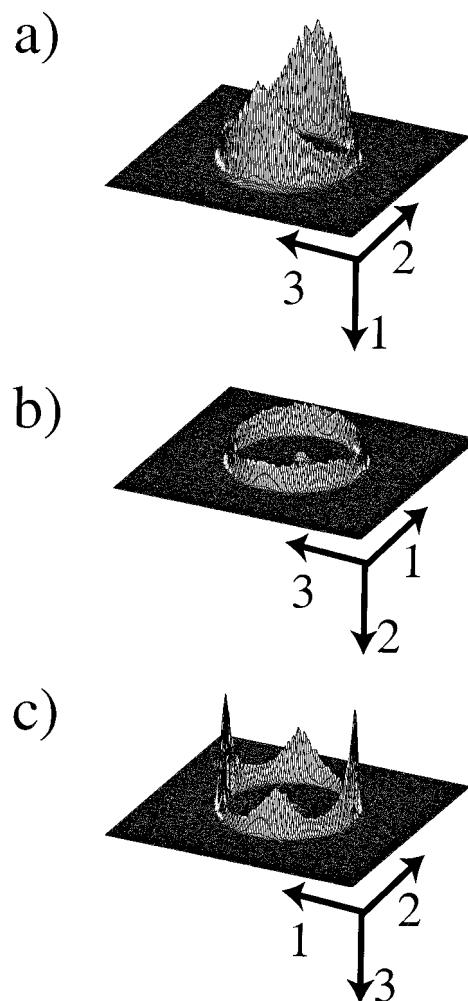
Figure 10. SAXS intensities in (a) tangential, (b) normal, and (c) radial views after oscillating P4VP(PDP)$_{1.0}$ for 15 h at 0.5 Hz, 56 °C, and 100% strain amplitude. Clear peaks in the 2-direction in (a) and (c) show the alignment to be parallel.

Figure 11. SAXS intensities in (a) tangential, (b) normal, and (c) radial views after oscillating P4VP(PDP)$_{1.0}$ at 10 Hz, 63 °C, and 100% strain amplitude for 22 h. Part (a) displays broad peaks in the 2-direction, indicating parallel alignment. Part (c) shows four peaks, two corresponding to parallel alignment and two in the 1-direction, corresponding to transverse alignment. The material still contains isotropic regions, as the large background in all three views indicates.

results of side chain liquid crystalline polymers is difficult because the value of the critical frequencies for these systems are not known. A *c* or "perpendicular" orientation has been reported, using a frequency of 100 rad/s and a strain amplitude of at least 50%.[30] For P4VP(PDP)$_{1.0}$ a smaller frequency of 0.5 Hz at 63 °C and a strain amplitude of 100% give the same result (see Figure 11). Even though the experiments of ref 30 were carried out well above the linear regime, which is around 1% for the side chain liquid crystalline material, with strains smaller than 50% there was no effect. For our material, shear alignment takes place even in the linear regime. This indicates that the mechanisms underlying the orientation behavior are different for both materials.

There is a considerable difference between different side chain liquid crystalline polymers: In some materials a high amount of orientation was obtained,[30] while in other cases the sample remained turbid throughout the shearing process, indicating a high density of defects.[52] Using the same parameters as in ref 30 for P4VP(PDP)$_{1.0}$ would in our case result in a poorly

parallel oriented material, as the result at 10 Hz and 100% strain amplitude at 56 °C for 22 h already indicates. Here, inhomogeneities could reduce the amount of orientation as well as causing the material sometimes to flow out of the sample holder. Alternatively, at these high frequencies the hydrogen bonds might break, leading to polymer backbones flowing in a sea of side chain solvent. The lamellar structure can no longer be maintained, and no alignment is possible. When the material is cooled to room temperature, these bonds are restored, resulting in isotropic lamellar material.

The orientation process of the side chain liquid crystalline polymers appears much faster, typically 12−20 min,[30,44,52] as compared to several hours for P4VP-(PDP)$_{1.0}$. It was observed that, upon cooling from the isotropic phase to the nematic phase while oscillating the material at various strain amplitudes, a dramatic change from an opaque, intensely scattering medium into a transparent and highly birefrigent material occurred already after 100−600 s of shear.[44,52] The induced alignment, however, was not stable, and part of the transparency was lost after the cessation of the shear.
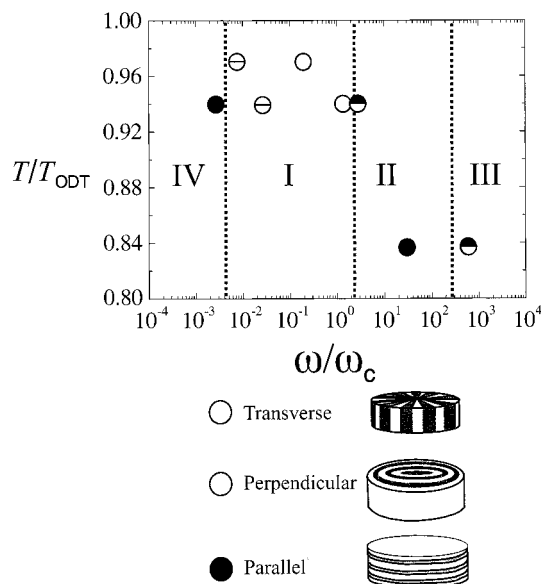
Figure 12. Alignment diagram of supramolecular comb copolymer P4VP(PDP)$_{1.0}$, i.e., reduced temperature (T/T_{ODT}) vs ω/ω_c, mapping the orientation observed after oscillating. Data are time−temperature shifted to $T_0 = 61$ °C. The dots indicate the alignment found at the current temperature and frequency. In region II, III, and IV parallel alignment was observed and in region I perpendicular alignment. A pure transverse alignment was found in the linear regime of region I. In region II the orientation flipped with time. In region I the orientation flipped from transverse to perpendicular with strain amplitude.

Finally, unlike an ordinary, i.e., covalently bonded, comb copolymer, where the polymer backbone might be stretched because of the conformational entropy, the side chains in the supramolecular comb copolymer P4VP(PDP)$_{1.0}$ are not permanently attached to the backbone, due to the dynamic nature of the hydrogen bonds. This allows for additional freedom of movement of the comb copolymer complex. Because of the comb architecture, and because the thickness of the P4VP-rich corresponds to a few polymer backbones only, the amphiphile-rich layer will be easily interpenetrated when the polymer backbones move, leading to undulations in the lamellae. Therefore, P4VP(PDP)$_{1.0}$ systems contain a lot of defect structures, resulting in broad SAXS peaks.

5. Conclusion

Comb-shape supramolecules, constructed by hydrogen bonding P4VP with a stoichiometric amount of pentadecylphenol (PDP), i.e., P4VP(PDP)$_{1.0}$, self-organize into a lamellar morphology. Dynamically oscillating P4VP-(PDP)$_{1.0}$ over a broad range of frequencies (0.001−10 Hz) renders four different alignment regimes, where the alignment was either parallel (II, III, and IV) or perpendicular (I) (see Figure 12). Moreover, it was possible to obtain a pure transverse alignment in the linear regime of region I. But even at 100% strain amplitude and 0.01 Hz at 63 °C, transversely aligned lamellae were still present.

Region II showed rich flipping phenomena from parallel to perpendicular to parallel as a function of time, at frequencies close to but above ω_c.

In region IV, the material orients transverse en route to parallel alignment. Here, because both blocks cannot relax, the material behaves as hard plates in a liquid. The material becomes turbulent at high frequencies,

and as a result defects are introduced, resulting in poorly parallel oriented material.

The behavior of the supramolecular comb copolymer P4VP(PDP)$_{1.0}$ has similarities with block copolymers, as demonstrated using the PS-*block*-PI diblock copolymer. It shows similar functional dependence of the shear moduli on the frequency and oscillating time and has a related shear alignment diagram. All regions were also found for PS-*block*-PI. In region IV, however, parallel alignment could only be obtained for annealed PS-*block*-PI diclock copolymers; for unannealed PS-*block*-PI perpendicular alignment was found. This requirement does not hold for our material, as our results at 0.001 Hz at 63 °C with unannealed P4VP(PDP)$_{1.0}$ have shown (see Figure 7). Despite the similarities, the underlying mechanisms seem different in regions I and II, as indicated by the flipping phenomena and the transverse/perpendicular biaxial alignments. Finally, a comparison with side chain liquid crystalline polymers, which resemble our comb copolymer architecture, shows that there it is possible to obtain macroscopically oriented material in a shorter time.

The rich orientational behavior of P4VP(PDP)$_{1.0}$, with its similarities as well as subtle differences with both block copolymers and side chain liquid crystalline polymers, not only makes this material a good alternative to block copolymers and side chain liquid crystalline polymers but also can open routes to new scientific investigations and applications.

References and Notes

(1) Alivisatos, A. P.; Barbara, P. F.; Castleman, A. W.; Chang, J.; Dixon, D. A.; Klein, M. L.; McLendon, G. L.; Miller, J. S.; Ratner, M. A.; Rossky, P. J.; Stupp, S. I.; Thompson, M. E. *Adv. Mater.* **1998**, *10*, 1297.
(2) Hamley, I. W. *The Physics of Block Copolymers*; Oxford University Press: Oxford, 1998.
(3) Bates, F. S.; Fredrickson, G. H. *Annu. Rev. Phys. Chem.* **1990**, *41*, 525.
(4) Fredrickson, G. H.; Bates, F. S. *Annu. Rev. Mater. Sci.* **1996**, *26*, 501.
(5) *Mechanical and Thermophysical Properties of Polymer Liquid Crystals*, 1st ed.; Brostow, W., Ed.; Chapman & Hall: London, 1998.
(6) Muthukumar, M.; Ober, C. K.; Thomas, E. L. *Science* **1997**, *277*, 1225.
(7) Duglosz, J.; Folkes, M. J.; Keller, A. *J. Polym. Sci., Part B: Polym. Phys.* **1973**, *11*, 929.
(8) Folkes, M. J.; Keller, A. *J. Polym. Sci., Part B: Polym. Phys.* **1976**, *13*, 833.
(9) Hadziioannou, G.; Mathis, A.; Skoulios, A. *Colloid Polym. Sci.* **1979**, *257*, 136.
(10) Koppi, K. A.; Tirrell, M.; Bates, F. S.; Almdal, K.; Colby, R. H. *J. Phys II* **1992**, *2*, 1941.
(11) Koppi, K. A.; Tirrell, M.; Bates, F. S. *Phys. Rev. Lett.* **1993**, *70*, 1449.
(12) Winey, K. I.; Patel, S. S.; Larson, R. G.; Watanabe, H. *Macromolecules* **1993**, *26*, 2542.
(13) Winey, K.; Patel, S. S.; Larson, R. G.; Watanabe, H. *Macromolecules* **1993**, *26*, 4373.
(14) Kannan, R. M.; Kornfield, J. A. *Macromolecules* **1994**, *27*, 1177.

(15) Gupta, V. K.; Krishnamoorti, R.; Kornfield, J. A.; Smith, S. D. *Macromolecules* **1995**, *28*, 4464.

(16) Zhang, Y.; Wiesner, U. *J. Chem. Phys.* **1995**, *103*, 4784.

(17) Zhang, Y.; Wiesner, U.; Spiess, H. W. *Macromolecules* **1995**, *28*, 778.

(18) Arendt, B. H.; Krishnamoorti, R.; Kannan, R. M.; Seitz, K.; Kornfield, J. A.; Roovers, J. *Macromolecules* **1997**, *30*, 1138.

(19) Chen, Z.-R.; Issaian, A. M.; Kornfield, J. A.; Smith, S. D.; Grothaus, J. T.; Satkowski, M. M. *Macromolecules* **1997**, *30*, 7096.

(20) Chen, Z.-R.; Kornfield, J. A.; Smith, S. D.; Grothaus, J. T.; Satkowski, M. M. *Science* **1997**, *277*, 1248.

(21) Maring, D.; Wiesner, U. *Macromolecules* **1997**, *30*, 660.

(22) Sänger, J.; Gronski, W.; Leist, H.; Wiesner, U. *Macromolecules* **1997**, *30*, 7621.

(23) Zhang, Y.; Wiesner, W. *Macromol. Chem. Phys.* **1998**, *199*, 1771.

(24) Chen, Z.-R.; Kornfield, J. A. *Polymer* **1998**, *39*, 4679.

(25) Leist, H.; Geiger, K.; Wiesner, U. *Macromolecules* **1999**, *32*, 1315.

(26) Wang, H.; Newstein, M. C.; Krishnan, A.; Balsara, N. P.; Garetz, B. A.; Hammouda, B.; Krishnamoorti, R. *Macromolecules* **1999**, *32*, 3695.

(27) Osuji, C.; Zhang, Y.; Mao, G.; Ober, C. K.; Thomas, E. L. *Macromolecules* **1999**, *32*, 7703.

(28) Safinya, C. R.; Sirota, E. B.; Bruinsma, R. F.; Jeppesen, C.; Plano, R. J.; Wenzel, L. J. *Science* **1993**, *261*, 588.

(29) Kannan, R. M.; Kornfield, J. A.; Schwenk, N.; Boeffel, C. *Macromolecules* **1993**, *26*, 2050.

(30) Hamley, I. W.; Davidson, P.; Gleeson, A. J. *Polymer* **1999**, *40*, 3599.

(31) Finkelmann, H.; Naegele, D.; Ringsdorf, H. *Makromol. Chem.* **1979**, *180*, 803.

(32) Volino, F.; Martins, A. F.; Blumstein, R. B.; Blumstein, A. *J. Phys. (Paris)* **1981**, *42*, 305.

(33) Noel, C.; Monnerie, L.; Achard, M. F.; Hardouin, F.; Sigaud, G.; Gasparoux, H. *Polymer* **1981**, *22*, 578.

(34) Lehn, J.-M. *Supramolecular Chemistry*; 1st ed.; VCH: Weinheim, 1995.

(35) Ruokolainen, J.; ten Brinke, G.; Ikkala, O.; Torkkeli, M.; Serimaa, R. *Macromolecules* **1996**, *29*, 3409.

(36) Ruokolainen, J.; Torkkeli, M.; Serimaa, R.; Komanschek, B. E.; ten Brinke, G.; Ikkala, O. *Macromolecules* **1997**, *30*, 2002.

(37) Ruokolainen, J.; Tanner, J.; Ikkala, O.; ten Brinke, G.; Thomas, E. L. *Macromolecules* **1998**, *31*, 3532.

(38) Antonietti, M.; Conrad, J.; Thünemann, A. *Macromolecules* **1994**, *27*, 6007.

(39) Ober, C.; Wegner, G. *Adv. Mater.* **1997**, *9*, 17.

(40) Mäkinen, R.; Ruokolainen, J.; Ikkala, O.; de Moel, K.; ten Brinke, G.; De Odorico, W.; Stamm, M. *Macromolecules* **2000**, *33*, 3441.

(41) Gupta, V. K.; Krishnamoorti, R.; Chen, Z.-R.; Kornfield, J. A.; Smith, S. D.; Satkowski, M. M.; Grothaus, J. T. *Macromolecules* **1996**, *29*, 875.

(42) Gupta, V. K.; Krishnamoorti, R.; Kornfield, J. A.; Smith, S. D. *Macromolecules* **1996**, *29*, 1359.

(43) Gupta, J. A.; Singh, M. A.; Salomons, G. J.; Foran, W. A.; Capel, M. S. *Macromolecules* **1998**, *31*, 3109.

(44) Kannan, R. M.; Kornfield, J. A.; Schwenk, N.; Boeffel, C. *Adv. Mater.* **1994**, *6*, 214.

(45) Safinya, C. R.; Sirota, E. B.; Plano, R. J. *Phys. Rev. Lett.* **1991**, *66*, 1986.

(46) Wiberg, G.; Skytt, M.-L.; Gedde, U. W. *Polymer* **1998**, *39*, 2983.

(47) Bates, F. S.; Koppi, K. A.; Tirrell, M.; Almdal, K.; Mortensen, K. *Macromolecules* **1994**, *27*, 5934.

(48) Wiesner, U. *Macromolecul. Chem. Phys.* **1997**, *198*, 3319.

(49) Chen, S. H.; Conger, B. M.; Mastrangelo, J. C.; Kende, A. S.; Kim, D. U. *Macromolecules* **1998**, *31*, 8051.

(50) Okamoto, S.; Saijo, K.; Hashimoto, T. *Macromolecules* **1994**, *27*, 5547.

(51) Zhang, Y.; Wiesner, U.; Yang, Y.; Pakula, T.; Spiess, H. W. *Macromolecules* **1996**, *29*, 5427.

(52) Rubin, S.; Kannan, R. M.; Kornfield, J. A.; Boeffel, C. *Macromolecules* **1995**, *28*, 3521.

(53) Noirez, L.; Lapp, A. *Phys. Rev. Lett.* **1997**, *78*, 70.

(54) Pinheiro, B. S.; Hajduk, D. A.; Gruner, S. M.; Winey, K. I. *Macromolecules* **1996**, *29*, 1482.

(55) Pinheiro, B. S.; Winey, K. I. *Macromolecules* **1998**, *31*, 4447.

(56) Patel, S. S.; Larson, R. G.; Winey, K. I.; Watanabe, H. *Macromolecules* **1995**, *28*, 4313.